Electronic Supplementary Material (ESI) for Physical Chemistry Chemical Physics.

ELECTRONIC SUPPORTING INFORMATION

High thermal sensitivity and selectable upconversion color of Ln, Yb:$Y_6O_5F_8$ nanotubes

Carlos Zaldo and Concepción Cascales*

Instituto de Ciencia de Materiales de Madrid, Consejo Superior de Investigaciones Científicas. c/ Sor Juana Inés de la Cruz 3, E-28049 Madrid, Spain. *ccascales@icmm.csic.es

Table S1. Selected bond distances lengths (Å) for $Y_6O_5F_8$ *

Y1-O1 2.2582 × 2	Y2-O1 2.2215	Y3-O2 2.3144	Y4-O3 2.2422 × 2
Y1-O1 2.3024 × 2	Y2-O1 2.3222	Y3-O2 2.2530	Y4-O3 2.2971 × 2
Y1-F2 2.2960 × 2	Y2-O2 2.2663	Y3-O3 2.2920	Y4-F1 2.2422 × 2
Y1-F2 2.5616 × 2	Y2-O2 2.2651	Y3-O3 2.2543	Y4-F1 2.2971 × 2
	Y2-F2 2.2918	Y3-F1 2.2920	Y4-F4 2.5382 × 2
Y1-Y1 3.6079 × 2	Y2-F3 2.3997	Y3-F1 2.2543	Y4-F5 2.2055
Y1-Y2 3.6084 × 2	Y2-F3 2.2842	Y3-F3 2.3527	Y4-F5 2.2951
Y1-Y2 3.8305 × 2		Y3-F4 2.2499	
	Y2-Y2 3.5761 × 2	Y3-F4 2.3112	Y4-Y4 3.5926 × 2
	Y2-Y3 3.5914		
	Y2-Y3 3.7277	Y3-Y3 3.5788 × 2	
		Y3-Y4 3.5730	
		Y3-Y4 3.6667	

* Unit cell parameters of $Y_5O_6F_8$: a = 5.415(6) Å, b = 33.133(8) Å, c= 5.530(4) Å, V = 992.17 Å^3. Space group *Pcmb* (57).[1].

Preparation of Er, Yb:β-$NaYF_4$

A 2 mol% Yb, 1 mol% Er:β-$NaYF_4$ (7 mmol) sample was synthesized by adding a previously prepared solution of Ln-nitrates (see main text) to a clear ethanolic solution (10 ml of ethanol (Emplura Merck) and 20 ml of distilled water) of NaF (Alfa-Ventron, 99 %), NaF:Ln=4:1. The formed turbid suspension was stirred and its pH was adjusted to 4 by adding HF (Merck 48 %), and then treated at 185 ºC for 24 h in a Teflon-lined autoclave. The product resultant of the hydrothermal treatment was collected by centrifugation and washed with ethanol several times, and overnight dried at 150 ºC in a desiccator. No need of further annealing was required to obtain the pure expected crystalline phase isostructural to hexagonal $P6_3/m$ (S. G. 176) β-$NaYF_4$ (JCPDS File #16-0334). However, it was subjected to a short annealing at 300 ºC to promote its better crystallization.

XPS analysis of Pr, Er, Yb:$Y_6O_5F_8$

Figure S1 shows the relevant parts of XPS obtained for $Y_{5.772}Yb_{0.12}Er_{0.003}Pr_{0.105}O_5F_8$. Adventitious carbon observed was used to normalize the binding energy scale, taken as reference the C 1s binding energy, 284.6 eV. Signals from all majoritary elements of the sample, i.e. Y, O and F, were detected. Yttrium 3d and 3p doublets are clearly observed in Figures S1a and S1b, respectively. In the first case the XPS spectrum shows two overlapped contributions associated to $3d_{5/2}$ and $3d_{3/2}$ electron emissions, and it was fit with peaks at 157.4 and 159.4 eV. Further Y peaks observed at 300.8 and 312.7 eV correspond to $3p_{3/2}$ and $3p_{1/2}$ emissions, respectively. The above binding energies agree those found in Y-oxide and Y-fluoride compounds,[2,3,4] see Table S2, and confirm exclusively the trivalent ionization state of Y in $Y_6O_5F_8$. Regarding oxygen, two overlapped peaks associated to O 1s level are observed in Figure S1c. This structure was fit with two components at 529.1 and 531.6 eV. Since in the $Y_6O_5F_8$ crystalline structure oxygen is exclusively bonded to Y, only one peak is expected. We ascribe the

peak at 529.1 eV to the oxygen in the oxyfluoride host, and the peak at 531.6 eV to oxygen contamination of the sample (absorbed atmospheric CO_2 and/or water), which is commonly found in the literature.[1] F 1s XPS signal in $Y_6O_5F_8$ peaks at 684.8 eV. The chemical shift of the binding energy is related to the inverse of the bond distance.[5] Taking into account that the average Y-O and Y-F bond distances in $Y_6O_5F_8$ are 2.27 Å and 2.35 Å (Table S1 in the Supporting Information), respectively, the O 1s and F 1s peaks of in $Y_6O_5F_8$ are expected at ≈529.5 eV and between 684.5-685 eV, respectively. This justifies our previous assignment of the O 1s binding energy and confirms the F 1s assignment, see Table S2.

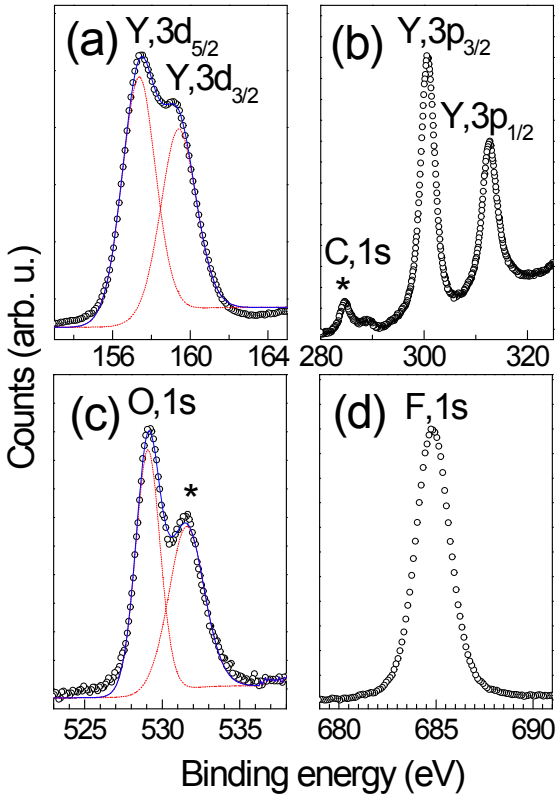

Figure S1. Spectra of (a) Y 3d, (b) Y 3p, (c) O 1s and (d) F 1s XPS peaks in $Y_6O_5F_8$. The points are the experimental results, the dashed lines the individual contributions to overlapped peaks and the continuous line the convolution of the above mentioned contributions. Adventitious C and O contaminations are marked with asterisks.

Table S2. Comparison of binding energies (in eV) in yttrium sesquioxide Y_2O_3, yttrium oxyfluorides YOF and $Y_6O_5F_8$, and yttrium trifluoride YF_3.

	Y^{3+}				O^{2-}	F^-	Ref
	3d5/2	3d3/2	3p5/2	3d3/2	1s	1s	
$Y_6O_5F_8$	157.4	159.4	300.8	312.7	529.1	684.8	this work
Y_2O_3	156.8	158.9			530.0		(42)
YOF	157.6		301.0	312.8	529.9-532.7	685.7	(43)
YF_3	158.9						(44)

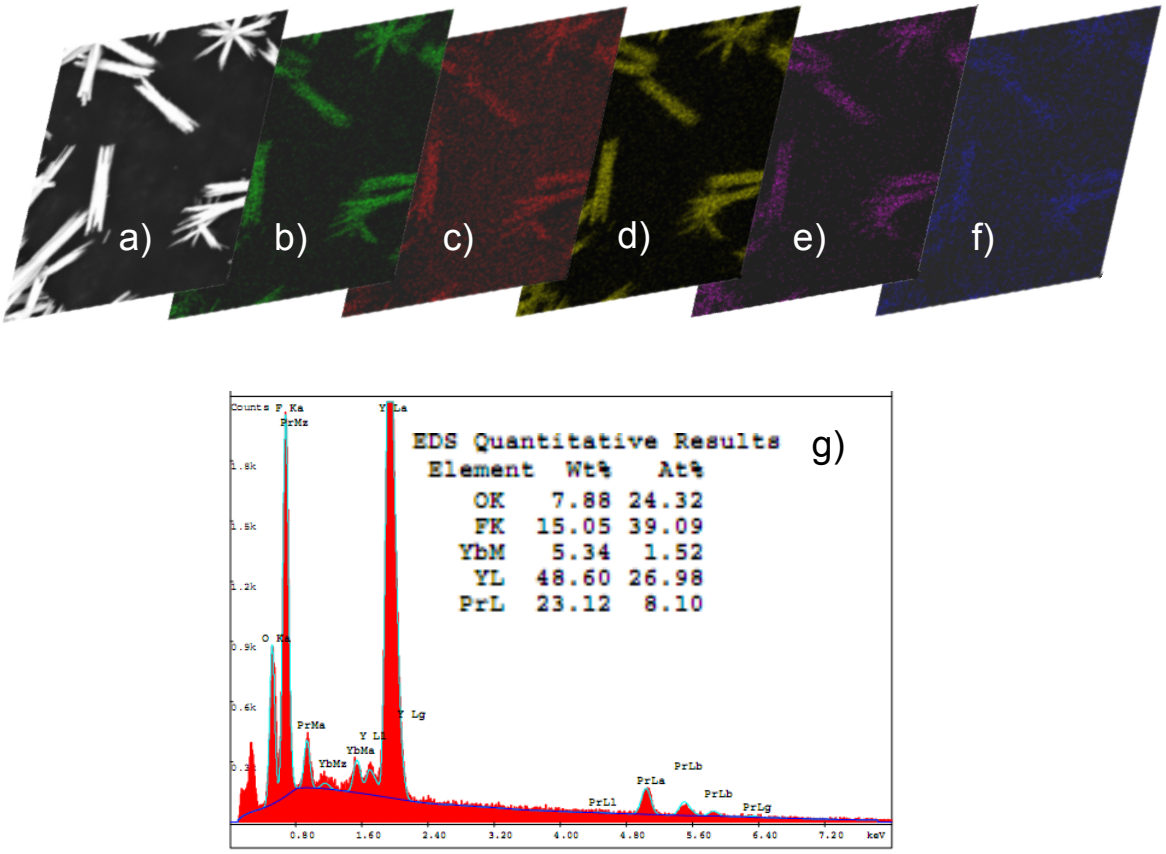

Figure S2. a) Field-emission SEM image of prepared $Y_{4.08}Yb_{0.12}Pr_{1.8}O_5F_8$. EDX color maps of: b) F, c) O, d) Y, e) Pr and f) Yb, showing the homogeneous distribution of these constitutive elements in formed nano/microtubes. g) Quantitative results.

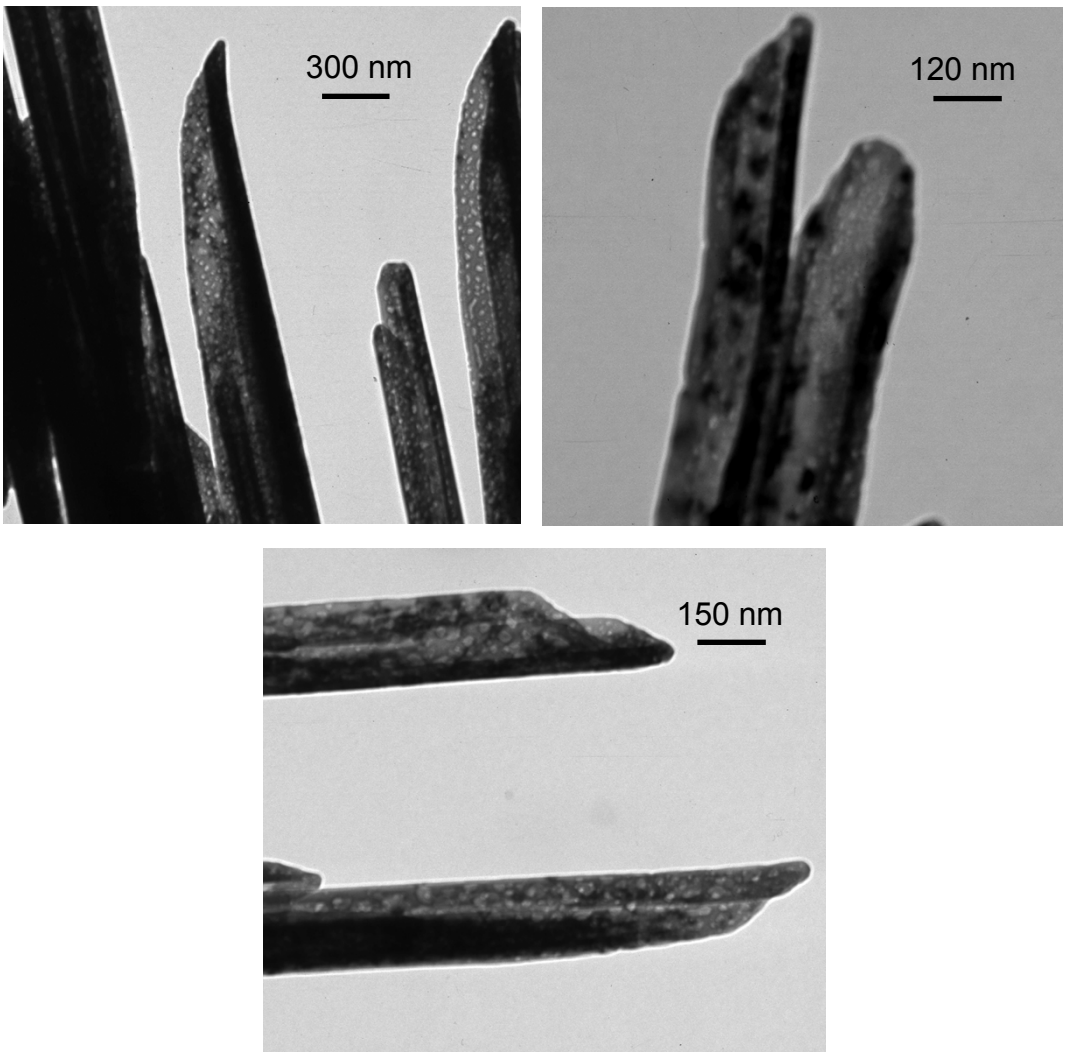

Figure S3. Additional TEM images of scrolls of Ln, Yb:$Y_6O_5F_8$ oxyfluorides rolled at different degrees.

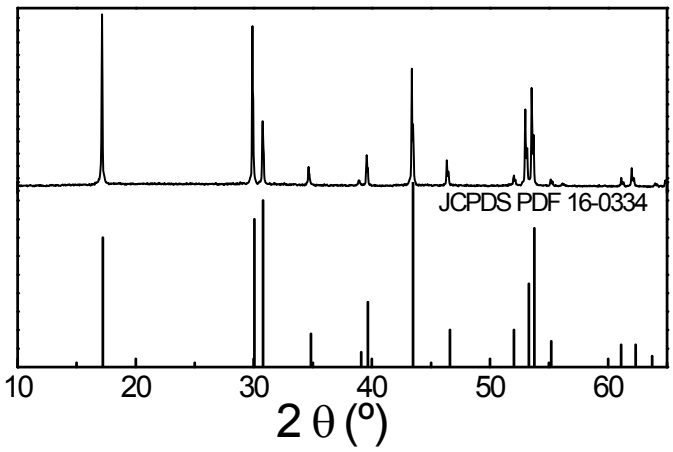

Figure S4. X-ray powder diffraction pattern of Er (1 mol%), Yb (2 mol%):β-$NaYF_4$ prepared from hydrothermal synthesis at 185 ºC. For comparison, the pattern scheme of hexagonal $P6_3/m$ (176) β-$NaYF_4$ JCPDS File 16-0334 has been also included in f).

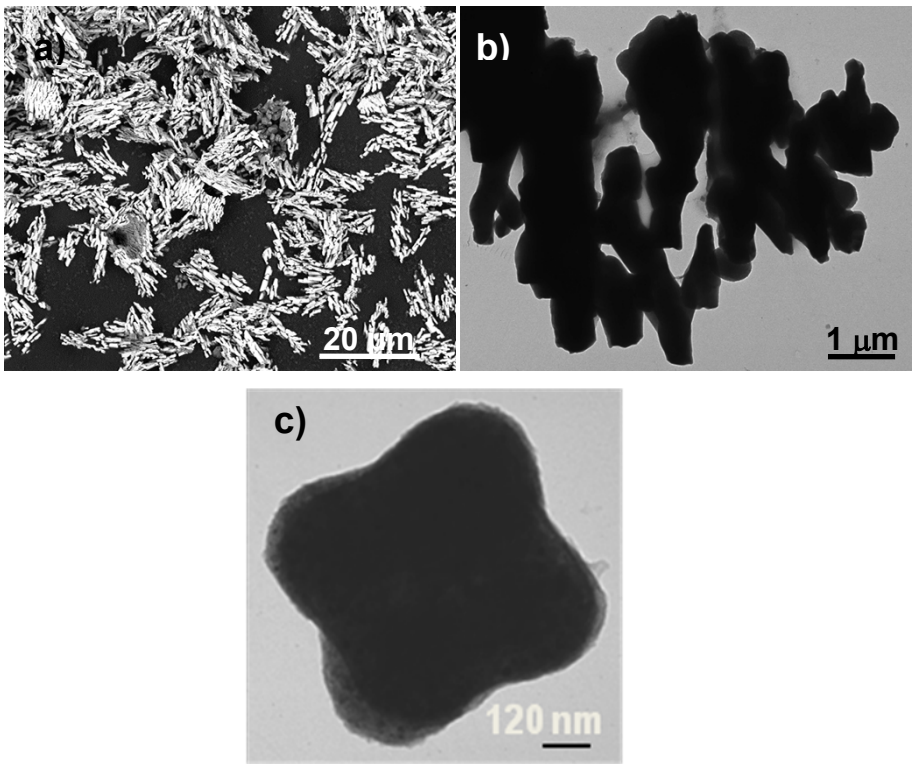

Figure S5. SEM a) and TEM b) and c) images of Er, Yb:β-$NaYF_4$ prepared by hydrothermal synthesis at 185 ºC.

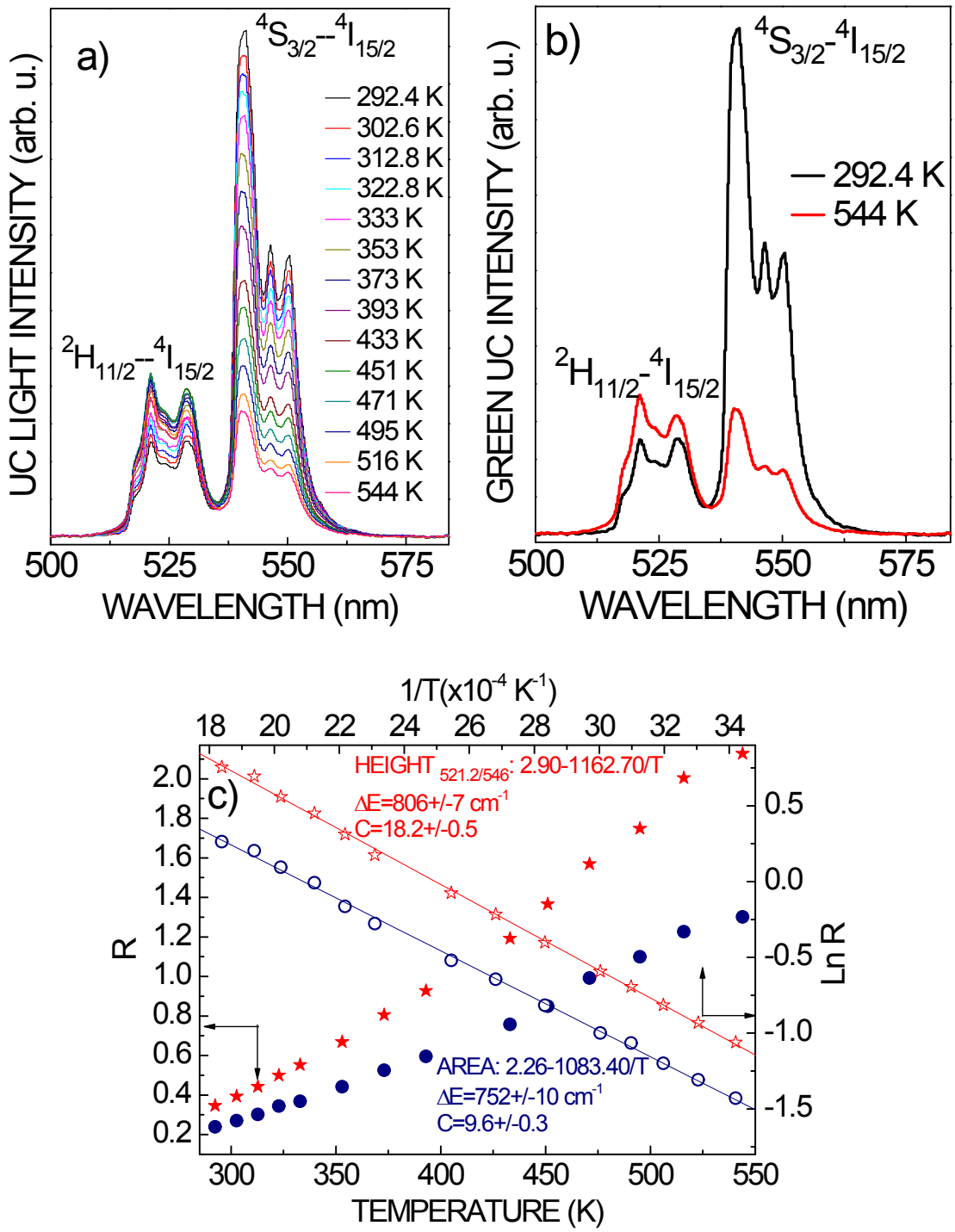

Figure S6. a) Evolution of NIR excited (λ_{EXC}~978 nm) upconversion green bands corresponding to $^2H_{11/2}$,$^4S_{3/2}$→$^4I_{15/2}$ electronic transitions of hydrothermal Er, Yb:β-$NaYF_4$ in the temperature range 292 K - 544 K. b) Comparison of upconversion green bands at 292 K and 544 K. c) Exponential dependence of R=$I^2H_{11/2}/I^4S_{3/2}$ with the temperature (full symbols). R values were measured as integrated areas of green Er^{3+} bands (circles), or as height of peaks at 521.2 nm ($^2H_{11/2}$) and 546 nm ($^4S_{3/2}$) (stars). From LnR vs 1/T plots (open symbols), best fits of above relationships were achieved (continuous lines). The first calibrating plot, 2.26-1083/T (R = 9.6·exp(-1083.4/T, open circles), and the derived value ΔE=752±10 cm^{-1}, are quite similar to the previously reported for microcrystalline 20 % Yb, 2% Er:β-$NaYF_4$, R=8.06·exp(-1082.1/T), with ΔE=752 cm^{-1},[6] for which the ratiometric analysis was also carried out from integrated areas of Er^{3+} green bands.

Optical absorption spectra and Pr^{3+} sites in Pr (30 mol%), Yb:$Y_6O_5F_8$

Room temperature and 6 K optical absorption spectra for Pr-doped Yb:$Y_6O_5F_8$ showing the transitions between the $^3H_4$ ground state and the excited multiplets $^3P_2$, $^1I_6$, $^3P_1$ and $^3P_0$ of the $4f^2$ Pr^{3+} configuration are presented in Figures S7a and S7b, respectively. The observed inhomogeneous broadening evidences overlapping of Pr^{3+} contributions due to the coexistence of different crystal fields around Pr^{3+} ions, which arise from four different point sites for Y^{3+} in the $Y_6O_5F_8$ crystal structure, see Table S1. Contributions corresponding to optical absorptions from $^3H_4$ to the next lying $^3P_1$ and $^1I_6$ multiplets are not clearly resolved at 6 K, thus any electronic transition involving these multiplets will be named as $^3P_1(+^1I_6)$ (see main text). However, four overlapped peaks can be distinguished along the band at ~480-490 nm corresponding to the absorption from $^3H_4(0)$ to the non-degenerate $^3P_0$ level, see the arrows in Figure S7b, which is in accordance with the four expected Pr^{3+} sites. The band peaking at 495 nm in the RT spectrum, marked with a star in Figure S7a, corresponds to optical absorptions arising from thermally populated excited levels of $^3H_4$, and almost disappears at 6 K, as can be seen in Figure S7b.

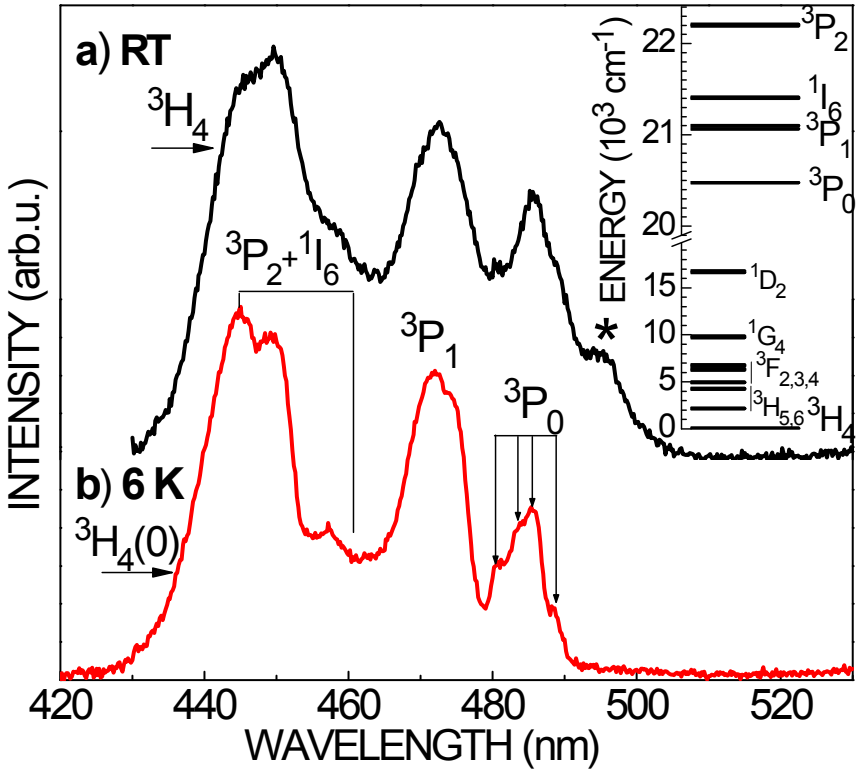

Figure S7. Optical absorption spectra of Pr^{3+} in Pr (30 mol%), Yb:$Y_6O_5F_8$ at: a) room temperature, and b) 6 K. The inset underlines the distribution of involved upper $^3P_2$, $^1I_6$, $^3P_1$, $^3P_0$ and ground $^3H_4$ energy levels of Pr^{3+}.

(1) D. J. M Bevan, J. Mohyla, B. F Hoskins, R. J. Steen, *Eur. J. Sol. State Inorg. Chem.* 1990, **27**, 451-465
(2) Y. Uwamino, T. Ishizuka, H. Yamatera, *J. Electron Spectrosc. Relat. Phenom.*. 1984, **34***,* 67-78.
(3) Ryzhkov, M. V.; Gubanov, V.A.; Butzman, M. P.; Hagstrom, A. L.; Kurmaev, E. Z. *J. Electron Spectrosc. Relat. Phenom.* 1980, **21***,* 193-204.
(4) R. P. Vasquez, M. C. Foote, B. D. Hunt, *J. Appl. Phys.* 1989, **66***,* 4866-4877.
(5) V. I. Nefedov, N. P. Sergushin, J. V. Salyn, *J. Electron Spectrosc. Relat. Phenom.* 1976, **8***,* 81-84.
(6) S. Zhou, K. Deng, X. Wei, G. Jiang, C. Duan, Y. Chen, M. Yin, Opt. Commun. 2013, **291**, 138-142.